Structural properties, superconductivity, and magnetism of metallic hydrogen

B. I. Min and H. J. F. Jansen
Department of Physics and Astronomy, Northwestern University, Evanston, Illinois 60201

A. J. Freeman
Department of Physics and Astronomy, Northwestern University, Evanston, Illinois, 60201
and Center for Materials Science, Los Alamos National Laboratory, Los Alamos, New Mexico 87545
(Received 29 May 1984)

The electronic band structure and structural properties of paramagnetic metallic hydrogen in the simple cubic (sc), fcc, bcc, and hcp phases have been determined theoretically using our bulk full-potential total-energy linearized augmented-plane-wave method. In the density range corresponding to $1<r_s<2$ we find a phase transition from sc to hcp at high pressure which indicates the importance of the hcp structure in phase transformations of molecular hydrogen under pressure. Superconducting transition temperatures up to 250 K are predicted within the framework of the rigid-ion approximation. An analysis of the Stoner factor shows the expected magnetic instability in the low-density region.

I. INTRODUCTION

Wigner and Huntington[1] proposed that molecular solid hydrogen—the stable phase under normal conditions—may become unstable at high pressures and transform into a metallic phase. Since this proposal, many investigators have examined the possibility of the existence of this metallic phase. An interesting aspect of these studies is the exciting speculation about high-temperature superconductivity in metallic hydrogen. Ashcroft[2] has predicted that this phase would become a high-temperature superconductor, because in simple metals there is a tendency for the electron-phonon coupling constant to increase as the density of a system increases. If a stable metallic hydrogen phase exists, its density is likely to be among the highest of the simple metals ($r_s \leq 2$, where r_s is the atomic sphere radius in a.u.), which immediately raises the possibility of high-temperature superconductivity. Results of a number of different model calculations[3] for this material indicate values of T_c varying between 0.08 and 250 K.

Experimental evidence supporting the presence of a metal-insulator phase transition became available when Vereshchagin *et al.*[4] measured the dependence of the resistance of solid hydrogen as a function of pressure and reported a sharp drop in the resistivity by 6 orders of magnitude at a pressure of approximately 1 Mbar at $T=4.2$ K. They explained this change in resistivity as a consequence of the phase transition in solid hydrogen to a metallic phase.

From a theoretical point of view, there have been several efforts to clarify the nature of this phase transition using a total-energy approach.[5,6] However, in order to reliably predict the transition between these two phases, it is necessary to apply the same method to both systems. Due to the very low symmetry of molecular hydrogen (ortho-hydrogen has a $Pa3$ space group), any approach is of necessity, less straightforward for the molecular solid than for metallic hydrogen. The common theoretical approach for molecular hydrogen is to calculate the energetics as in an ordinary molecular solid using standard pair potentials, while for metallic hydrogen one employs a band-structure calculation or one considers perturbation theory applied to a uniform electron gas. As an example of a consistent approach to this problem one may cite the recent work by Chakravarty *et al.*[7] For metallic hydrogen they performed self-consistent band-structure calculations using the spherical Wigner-Seitz cell method. For molecular hydrogen they considered first the average potential in a Wigner-Seitz spherical cell and then used perturbation theory to include the intracellular molecular symmetry.

It is now commonly accepted that in the high-density region, metallic hydrogen is a paramagnetic metal, while at low densities it is a magnetic insulator probably with an antiferromagnetic structure. Recently, Rose *et al.*[8] discussed the metal-insulator transition of a hydrogen system in relation to the Mott transition using spin-density-functional theory. They did not consider any structural differences since they used the Wigner-Seitz cellular method with a spherical unit cell in their calculations and assumed the magnetic phase to have ferromagnetic symmetry. They found that there would be two separate phase transitions: a magnetic transition at $r_s=2.74$ and a metal-insulator transition at $r_s=2.84$.

Our approach is to perform electronic structure calculations with our self-consistent full-potential linearized augmented-plane-wave (FLAPW) method, which has been applied very successfully to molecules,[9] thin films,[10] and bulk materials.[11] Since the FLAPW method allows one to accurately consider both the metallic phase and the complicated $Pa3$ structure (with four molecules per unit cell which gives rise to large anisotropic molecular interactions), a direct, consistent comparison of the total energy for both phases will be possible for the first time using a method which does not resort to severe numerical approximations.

In this study, we report on the electronic structure of

 ©1984 The American Physical Society

metallic hydrogen and its resulting structure-dependent cohesive-energy properties. Usually one considers the fcc phase to be most stable in the region where the phase transition takes place. In order to assess this proposition we performed total-energy calculations for three cubic structures—fcc, bcc, and simple cubic (sc)—and for the hcp structure. The relative stability as a function of pressure is derived from total-energy calculations as a function of volume. We investigated the superconducting properties in the framework of the rigid-ion approximation, which although basically a very simplified model, is known to predict values for T_c fairly well even for the transition metals.[12] Since the rigid-ion approximation is known to underestimate T_c for non-transition-metals, the theoretical T_c values of ~ 250 K may be considered as a lower limit. The problem of magnetic phase transitions was investigated by monitoring the Stoner factor, which is easily obtained from the converged charge density and potential. The results of band-structure and total-energy calculations are presented in Sec. II. Superconductivity and magnetic properties are discussed in Sec. III. In Sec. IV we give a discussion and a summary.

II. BAND-STRUCTURE, TOTAL-ENERGY, AND STRUCTURAL PROPERTIES

We have obtained band structures and total energies of metallic hydrogen using the FLAPW method[11] within the local-density-functional theory. In this method we make no shape approximations in either the potential or the charge density and we carefully examine the convergence of the results with respect to all numerical parameters. Obviously, our calculations still depend on the local-density approximation and the choice of exchange and correlation potential, for which we employ the form of von Barth and Hedin[13] with the parameters of Hedin and Lundqvist[14] and random-phase approximation (RPA) scaling for the ferromagnetic results. However, these approximations relate to the physics of the problem and are totally different in nature from severe numerical approximations such as the use of the spherical Wigner-Seitz cellular method or other approaches.

First we consider the electronic structure of the fcc phase in the range $1.0 < r_s < 3.0$, where the charge density for each value of r_s is obtained self-consistently using 20 and 80 $\vec{k}$ points in the $\frac{1}{48}$th irreducible Brillouin zone (IBZ) and 65 LAPW basis functions at the Γ point. The potential and the charge density are expanded in lattice harmonics up to $l=8$ inside the muffin-tin sphere and in 537 plane waves in the interstitial region. In this manner we established a sufficiently converged accuracy with respect to the basis size and the number of nonspherical terms. We find that the values of the total energy (see Fig. 1), the curvature, and even the equilibrium position of the curve are very sensitive to the number of $\vec{k}$ points, because the Fermi surface of hydrogen has only electron parts and no cancellation of errors occurs.[11] Therefore, in order to obtain converged values for the total energy, it is essential to calculate the band structure with a large number of $\vec{k}$ points. We performed our calculations with increasing numbers of $\vec{k}$ points up to 160, 165, and 204 in the IBZ for the fcc, sc, and bcc structures, respectively. This allows us to extrapolate the total energy to its value for an infinite number of $\vec{k}$ points[11] with an accuracy better than 1 mRy for each value of r_s. The Fermi surface of hcp metallic hydrogen is considerably more complicated. It consists of two pieces originating from deformed free-electron spheres which now intersect along the Γ-A directions and both of which give rise to electronlike orbits. In the hcp case the effect on the total energy of errors in the description of the Fermi surface on the total energy due to a finite $\vec{k}$ mesh is even larger than in the case of the cubic structures. This leads to an error in the extrapolated value of the total energy of 2 mRy, as based on calculations using up to 150 $\vec{k}$ points. In this respect hydrogen is not a simple material since in transition metals the errors are usually much smaller.[11]

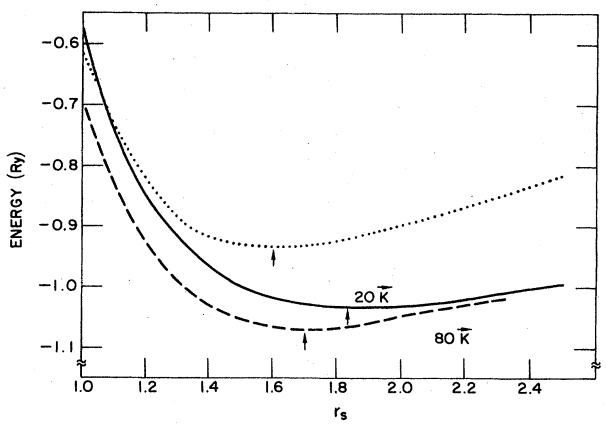

FIG. 1. Total-energy curve of fcc metallic hydrogen, calculated with 20 and 80 $\vec{k}$ points in an irreducible Brillouin zone (solid and dashed lines, respectively). The results of a jellium model calculation are also shown for comparison (dotted line).

The energy band structures of the cubic structures are very similar to free-electron bands; in fact, the Fermi surfaces of the fcc and bcc structures are almost the same as the Fermi sphere found in a free-electron-gas treatment. In the sc structure the Fermi surface crosses the boundary of the first Brillouin zone, giving rise to necks along the X axis.

The final value of the equilibrium atomic radius r_s^0, the ground-state energy E^0, and the bulk modulus are given in Table I. Figures 2 and 3 show that in the low-density region the sc structure is most stable, as was found before, but as the density increases, the hcp structure becomes stable. The fcc structure has the highest energy in the density range considered; this result is clearly different

TABLE I. Equilibrium Wigner-Seitz radius r_s^0, total energy E^0, and bulk modulus B^0 at r_s^0, as derived from a parabolic fit to values of the total energy near the equilibrium position.

	r_s^0 (a.u.)	E^0 (Ry)	B^0 (Mbar)
fcc	1.683	−1.0763	1.251
bcc	1.677	−1.0775	1.071
sc	1.707	−1.0878	1.123

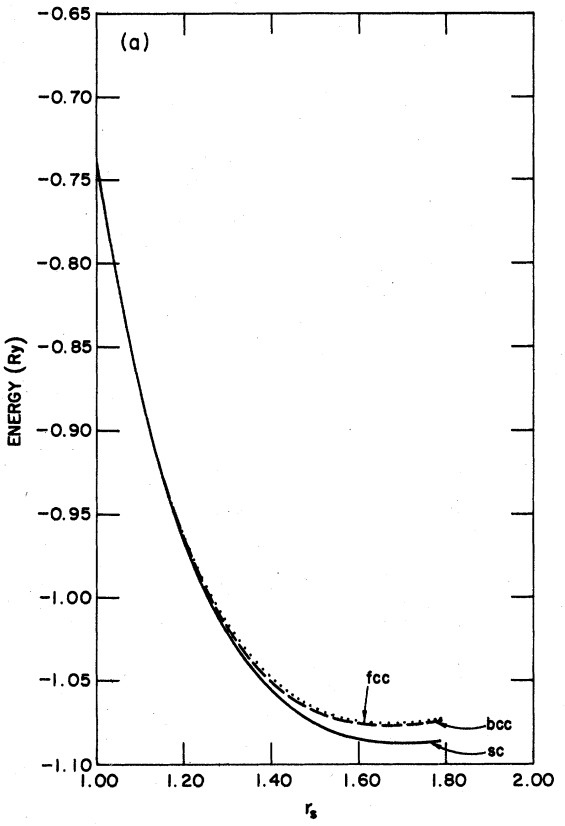

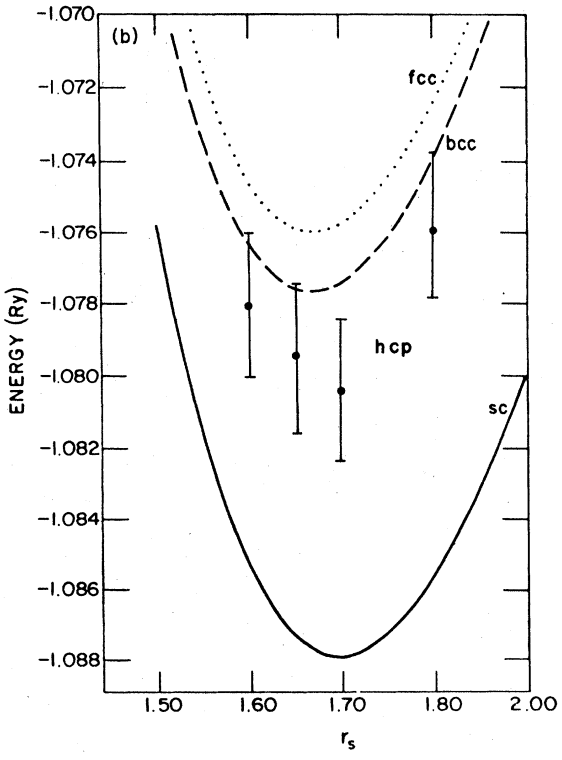

FIG. 2. (a) Total energy of metallic hydrogen vs r_s. (b) Enlarged plot of the total energy near the equilibrium values of r_s.

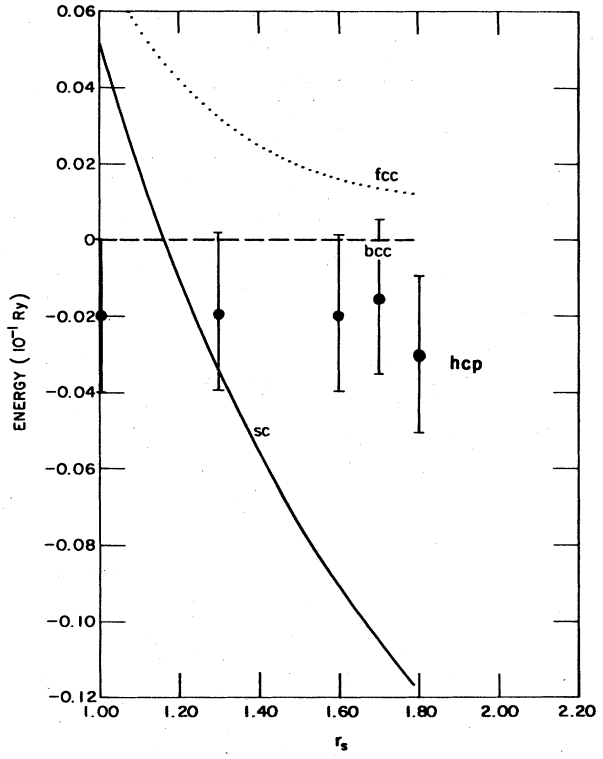

FIG. 3. Energy difference relative to the bcc structure for fcc, hcp, and sc metallic hydrogen as a function of the electronic density.

from earlier predictions.[6,15]

In order to obtain the pressure and Gibbs free energy, we fit the values of the total energy to an interpolating form derived from the Nozières-Pines[16] formula for the uniform electron gas:

$$E=\frac{2.21}{r_s^2}+\frac{A}{r_s}+B+C\ln r_s\ . \tag{1}$$

We have fixed the kinetic energy (first) term and have determined the parameters A,B,C by a least-squares fit with a root-mean-square error less than 1 mRy. The resulting parameters for the three cubic structures are given in Table II. (Note that the values for B and C as used by Nozières and Pines are -0.115 and 0.031, respectively.) From this relation, we obtain the pressure and Gibbs free energy, which are given in Tables III and IV and in Fig. 4. The transition pressure between the sc and bcc phases is 7.16 Mbar and the free energy at that point is -0.6155 Ry. We did not parametrize the hcp results by the formula given in Eq. (1), because the large increase in computing time required for this structure made possible only a

TABLE II. Parameters A, B, and C used in the interpolating formula [Eq. (1)] for the total energy.

	A	B	C
fcc	−2.796 21	−0.147 64	−0.090 76
bcc	−2.839 82	−0.111 42	−0.113 25
sc	−2.806 04	−0.139 93	−0.116 79

TABLE III. Energy and pressure as a function of the electronic density (1 a.u. of pressure is 147.08 Mbar).

	Energy (Ry)			Pressure (a.u.)		
r_s	fcc	bcc	sc	fcc	bcc	sc
1.0	−0.7339	−0.7412	−0.7360	0.1364	0.1348	0.1373
1.1	−0.8719	−0.8774	−0.8756	0.0718	0.0708	0.0726
1.2	−0.9596	−0.9639	−0.9649	0.0382	0.0376	0.0388
1.3	−1.0147	−1.0179	−1.0214	0.0201	0.0197	0.0206
1.4	−1.0479	−1.0504	−1.0560	0.0101	0.0099	0.0105
1.5	−1.0664	−1.0683	−1.0758	0.0045	0.0044	0.0048
1.6	−1.0746	−1.0763	−1.0853	0.0014	0.0013	0.0016
1.7	−1.0759	−1.0773	−1.0878	−0.0004	−0.0005	−0.0002
1.8	−1.0723	−1.0736	−1.0854	−0.0013	−0.0014	−0.0011

smaller number of data points. However, from Fig. 3 we immediately deduce that the phase transition between sc and hcp occurs just before the transition to bcc metallic hydrogen would take place.

It has been usually expected that the fcc phase would be more stable than the bcc phase in the density region near $r_s=1.0$. Instead, we find the bcc phase to be more stable than the fcc phase. This can be understood as a result of the inclusion of nonspherical anisotropic effects in the density and potential. In fact, similar calculations performed with the linearized muffin-tin orbital (LMTO) method[17] where a spherical potential is assumed, yield result which indicate that the fcc phase is more stable than bcc in the density region considered although energy differences are less than 1 mRy. Since the bcc and the sc structure are more open than the fcc close-packed structure, it is not surprising that the nonspherical terms are more important in these structures and that the total energy is lowered by a larger amount in bcc and sc metallic hydrogen when these nonspherical terms are included in the calculation.

We can understand the structural transformation between the sc, bcc, and hcp structures as follows. If we assume that the system is a point proton lattice embedded in a uniform electron gas (i.e., an inverse Wigner lattice), then the total energy is given by

$$E_T=\frac{2.21}{r_s^2}-\frac{0.916}{r_s}-0.115+0.031\ln r_s-\frac{A_M}{r_s}\ . \quad (2)$$

Originally, the Wigner lattice corresponds to the very-low-density electron gas. But we assume here only a situation similar to that of a Wigner lattice and use the Nozières and Pines interpolation formula for the correlation energy. Therefore the first four terms are uniform electron-gas results and the final term comes from the energy of point lattice charges in a uniform negative background—a kind of Madelung energy E_M. Only this Madelung energy depends on the structure: A_M's are 1.760 12, 1.791 75, 1.791 86, and 1.791 68 for the sc, fcc, bcc, and hcp structure, respectively.[18] Hence, the difference of our total-energy formula [Eq. (1)] from the above inverse Wigner lattice expression, E_b, can be considered as a band-structure effect (nonuniform electron distribution, etc.). If band effects are negligible, the dominant structur-

TABLE IV. Gibbs free energy as a function of pressure.

	G (Ry)		
P (a.u.)	fcc	bcc	sc
0	−1.0763	−1.0775	−1.0876
5×10^{-4}	−1.0667	−1.0681	−1.0780
1×10^{-3}	−1.0576	−1.0591	−1.0686
5×10^{-3}	−0.9957	−0.9978	−1.0050
1×10^{-2}	−0.9330	−0.9355	−0.9411
2×10^{-2}	−0.8306	−0.8338	−0.8374
3×10^{-2}	−0.7453	−0.7491	−0.7511
5×10^{-2}	−0.6024	−0.6071	−0.6069
1×10^{-1}	−0.3257	−0.3322	−0.3286

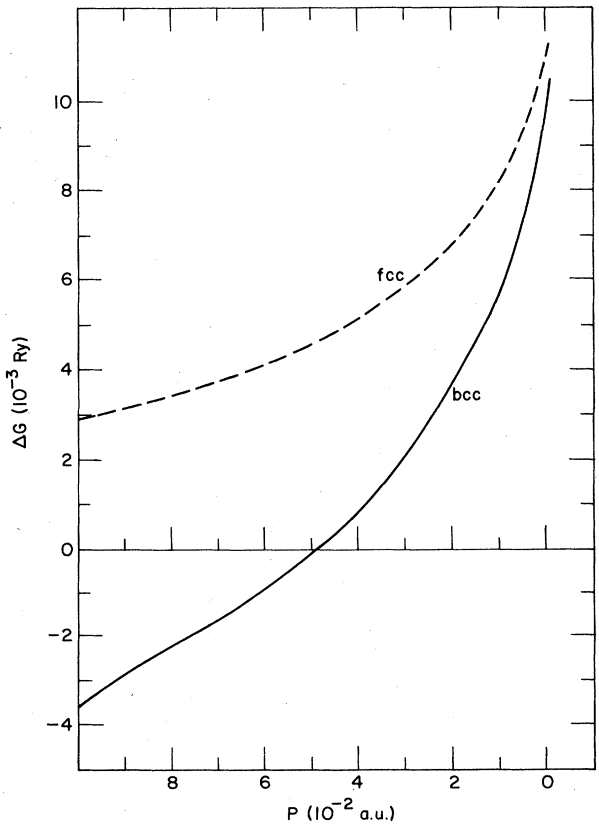

FIG. 4. Gibbs free-energy differences relative to the sc structure for fcc and bcc metallic hydrogen as a function of pressure.

TABLE V. Band-structure effect energy E_b, and the difference in E_b and the Madelung energy E_M between the bcc and sc structure. All energies are in Ry a.u.

	E_b				
r_s	fcc	bcc	sc	E_b(bcc-sc)	E_M(bcc-sc)
1.0	−0.1208	−0.1281	−0.1546	0.0265	−0.0317
1.1	−0.1244	−0.1299	−0.1569	0.0270	−0.0285
1.2	−0.1283	−0.1324	−0.1599	0.0275	−0.0265
1.3	−0.1324	−0.1355	−0.1634	0.0279	−0.0244
1.4	−0.1366	−0.1390	−0.1673	0.0283	−0.0227
1.5	−0.1408	−0.1427	−0.1713	0.0286	−0.0212
1.6	−0.1450	−0.1465	−0.1754	0.0289	−0.0198
1.7	−0.1491	−0.1504	−0.1796	0.0292	−0.0187
1.8	−0.1532	−0.1544	−0.1838	0.0294	−0.0176

al difference in energy comes from the Madelung term favoring the bcc structure as the most stable one. This implies the existence of a hcp-bcc phase transition at some density with $r_s < 1$.

Table V lists the band-structure effects and for comparison also the Madelung energy differences. These results show that in the density range considered, variations in the differences in band effect energy between sc and bcc are small compared with those in the Madelung energy differences. Therefore, in the low-density region, the band effect E_b is more important than the Madelung energy E_M, while in the high density, the situation is reversed.

III. SUPERCONDUCTING AND MAGNETIC PROPERTIES

In order to study the superconducting properties, we apply the rigid muffin-tin approximation[12] (RMTA) to our results for metallic hydrogen. In the RMTA, the change in potential is assumed to be given by rigidly displaced muffin-tin potentials. With this approximation and McMillan's strong-coupling theory,[19] the electron-phonon coupling constant λ is simply given by

$$\lambda = \frac{N(E_F)\langle I^2\rangle}{M\langle\omega^2\rangle} \equiv \eta/M\langle\omega^2\rangle \ , \tag{3}$$

$$\eta = \frac{2E_F}{\pi^2 N(E_F)} \sum_l (l+1)\sin^2(\delta_l - \delta_{l+1})\nu_l\nu_{l+1} \ , \tag{4}$$

with $N(E_F)$ representing the density of states per spin, $\langle I^2\rangle$ the electron-phonon matrix element, M the ionic mass, and $\langle\omega^2\rangle$ the average phonon frequency squared. Here, $\nu_l = N_l(E_F)/N_l^0(E_F)$, where $N_l(E_F)$ and $N_l^0(E_F)$ are partial densities of states per spin (obtained from angular-momentum projections inside the muffin tins) of

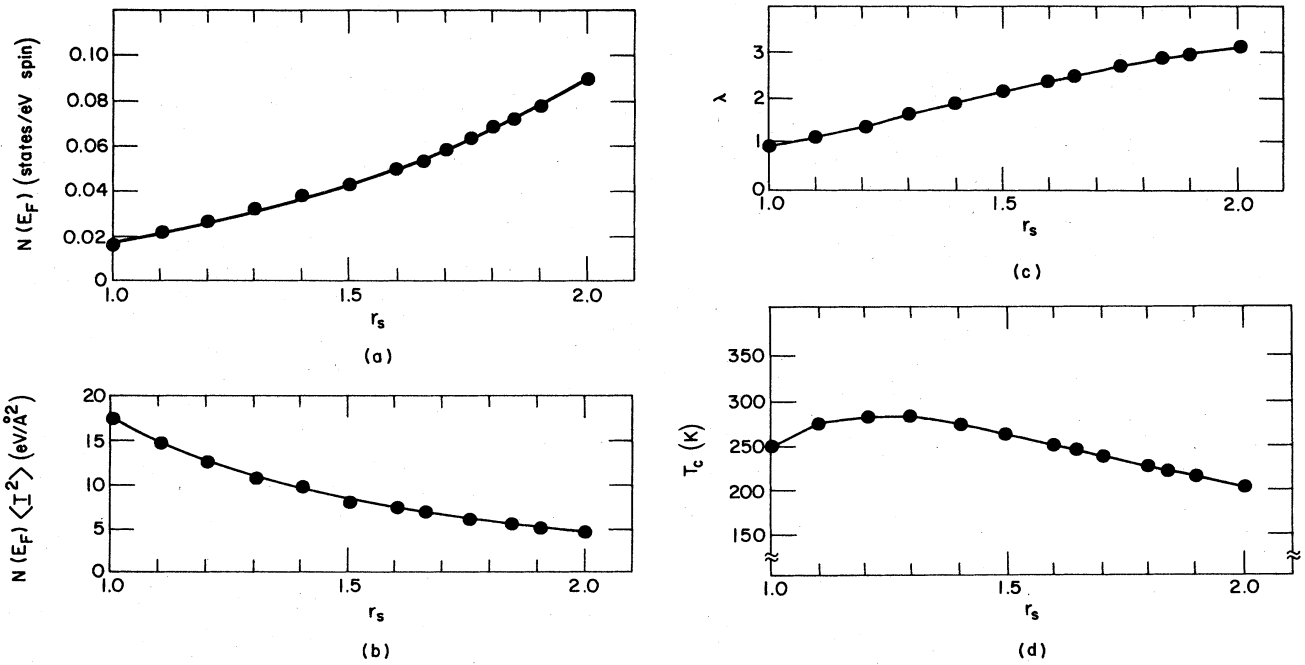

FIG. 5. Parameters entering into the description of the superconductivity of metallic solid hydrogen in the range $1.0 < r_s < 2.0$: (a) density of states per spin $N(E_F)$; (b) average electron-phonon matrix element $N(E_F)\langle I^2\rangle$; (c) electron-phonon coupling constant λ; and (d) superconducting transition temperature T_c.

TABLE VI. Electron-phonon coupling constant λ and superconducting transition temperature T_c for the fcc phase.

r_s	λ	T_c
1.0	0.965	243.3
1.1	1.168	267.2
1.2	1.390	276.9
1.3	1.631	276.9
1.4	1.889	270.9
1.5	2.164	261.7
1.6	2.400	248.1
1.7	2.800	242.0
1.8	2.953	225.7

a solid and of a single scatterer, respectively, and δ_l is the phase shift for the lth partial-wave scattering from the spherical muffin-tin potential. In strong-coupling theory, the superconducting transition temperature T_c is given by

$$T_c=\frac{\Theta_D}{1.45}\exp\left[-\frac{1.04(1+\lambda)}{\lambda-(1+0.62\lambda)\mu^*}\right] \quad (5)$$

with Θ_D the Debye temperature and μ^* the Coulomb pseudopotential parameter. We use $\mu^*=0.1$, which is a usual assumption for simple metals. Changing this value to $\mu^*=0.0255$ (as derived from the formula of Benneman and Garland[20]) increased the value of T_c by only 12%. For the Debye temperature Θ_D, we use the results of Caron's self-consistent harmonic phonon approximation:[21]

$$k\Theta_D=\frac{0.0453}{r_s^{3/2}}-\frac{0.023}{r_s^{1/2}}+0.006r_s^{1/2} . \quad (6)$$

The calculated T_c values are shown in Table VI and the relevant parameters in Fig. 5. These data pertain to the fcc phase; values for the bcc, sc, and hcp structures are very similar. The values of T_c and the other parameters are not sensitive to the values of Θ_D chosen. This means that the contribution from electronic effects is dominant and that possible errors from the use of Caron's formula are not very significant. Figure 5 shows that T_c increases above 200 K in the density range considered.

We have calculated the Stoner factor in order to investigate the magnetic properties of metallic hydrogen. With our paramagnetic results we can determine the intra-atomic exchange-correlation integral I_{xc} easily. The method of Jarlborg and Freeman[22] is used, with the local-spin-density-functional form of Gunnarsson and Lundqvist.[23] The Stoner factor S can be written in terms of the exchange-correlation integral I_{xc} as

$$S=[1-I_{xc}N(E_F)]^{-1} . \quad (7)$$

The values obtained for S for a number of r_s values are given in Table VII. To trace the magnetic instability, we fit these values with the RPA formula for χ^0/χ in the high-density limit:

$$\chi^0/\chi=1+Ar_s+Br_s^2+Cr_s^2\ln r_s . \quad (8)$$

The resulting values of the parameters A, B, and C are listed in Table VIII together with, for comparison, results for the uniform electron gas in the high-density limit.[24] The behavior of $1/S$ is shown in Fig. 6. As expected, we find an instability, occurring near $r_s=2.95$, 3.31, and 2.67 for fcc, sc, and bcc, respectively. These results are in good agreement with self-consistent calculations of Rose *et al.*[8] and are also confirmed by the preliminary results obtained in ferromagnetic calculations which are in progress.

TABLE VII. Stoner factors for some values of r_s.

r_s	fcc	bcc	sc
1.0	1.154	1.141	1.143
1.3	1.235	1.213	1.215
1.6	1.363	1.326	1.319
1.65	1.392	1.352	1.343
1.7	1.426	1.380	1.366
1.75	1.461	1.465	1.390
1.8	1.499	1.487	1.399
3.0	−1.487		

TABLE VIII. Parameters A, B, and C in the interpolation formula $\chi^0/\chi=1/S$ [Eq. (8)] and magnetic instability point $r_s^m(\chi^0/\chi\to 0)$. The electron-gas values in the high-density limit are also shown for comparison.

	A	B	C	r_s^m
fcc	−0.2398	0.1060	−0.1284	2.95
bcc	−0.4821	0.3556	−0.3212	2.67
sc	−0.1687	0.0434	−0.0696	3.31
electron gas	−0.1659	0.0290	−0.0138	6.6

IV. DISCUSSION

We have studied the cohesive properties of metallic hydrogen using the FLAPW method within local-density-functional theory. Even though the system is extremely simple, with one electron per atom, the total-energy calculations had to be performed with great care. It is essential to use a large number of $\vec{k}$ points in the self-consistency process in order to obtain good results. Fortunately, convergence to self-consistency does not require many iterations. As the number of $\vec{k}$ points increases, the time consumed for each iteration becomes correspondingly large.

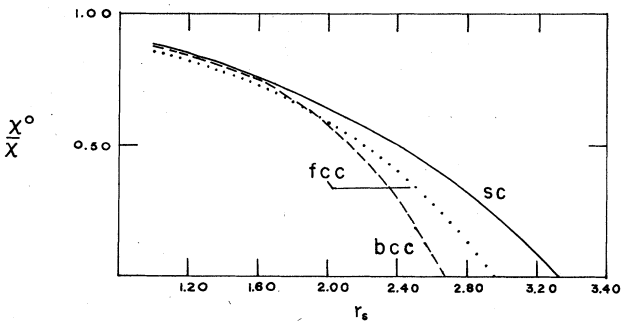

FIG. 6. Inverse Stoner parameter for metallic hydrogen derived from formula (8) in the text.

For this reason, we have used an extrapolation scheme based on the analytic error behavior of the linear tetrahedron method—an approach which proved to be satisfactory.[11]

This study was limited to the relative stability of the hcp, fcc, bcc, and sc phases because these structures are the most likely candidates for the ground state of metallic hydrogen. Confirming earlier predictions,[6] we find the sc phase to be most stable with a minimum in the total energy near $r_s = 1.7$. A similar ordering of the cubic phases is also found in diamond under pressure.[25] Of course, we do not predict that at this density solid hydrogen will be simple cubic, because the molecular $Pa3$ structure still has a lower energy. This indicates that the simple-cubic phase is likely to be unstable with respect to distortions along $\langle 111 \rangle$ axes which transform it to the $Pa3$ structure.

Our calculations show that at high pressures, corresponding to $r_s = 1.0$, metallic hydrogen occurs in the hcp modification, which is consistent with experimental data on Li and Na.[26] At even higher pressures, metallic hydrogen will have to transform to a bcc structure due to the dominating effects of the Madelung term for values of r_s close to zero. Whether the hcp phase will be experimentally observable depends on the position of the total-energy curve for molecular hydrogen with respect to the hcp and bcc structures. In contrast to earlier calculations, we find that the fcc phase does not play an important role at high densities. This is due to the correct treatment in our calculations of nonspherical terms in the density and the potential, the effects of such terms being smallest in the fcc case.

In resolving the question whether (if at all) molecular hydrogen at high pressure will transform into a bcc or hcp phase one also has to consider the contributions to the total energy due to changes in the phonon spectra.[7] The two important quantities in this respect are the plasma frequency and the wave-vector-dependent dielectric function. The plasma frequency is density dependent and it determines the overall energy scale of the proton motion; for the very light hydrogen atoms it results in changes of the binding energy on the order of 10 mRy.[7] Structure-dependent effects on the phonon energy are isolated in the dielectric function. Because of the strong similarity in band structure between the three cubic phases the relative ordering of these phases will hardly be affected. However, the band structure near the Fermi surface for hcp metallic hydrogen is different and might cause a sufficiently large change in total energy to reverse the ordering of bcc and hcp metallic hydrogen. Since the difference in total energy between the hcp and bcc phase of $r_s = 1$ is only 2 mRy; a 20% change in phonon energy would be sufficient to establish such a reversal. As already stated by Chakrvarty *et al.*,[7] phonon effects in molecular hydrogen will be even stronger, necessitating a full calculation of the $\vec{k}$-dependent dielectric function in order to accurately predict the pressure at which molecular hydrogen will transform to a metallic phase.

From an analysis of the Stoner factor we expect a magnetic transition to occur at lower densities. We are currently investigating the nature of the magnetic transition by a series of ferromagnetic and antiferromagnetic calculations based on local-spin-density-functional theory. Using the results of our paramagnetic calculations, we are able to predict values for the superconducting transition temperature well exceeding 200 K. Hence, assuming that one is experimentally able to transform molecular hydrogen to a simple metallic phase at a sufficiently high pressure, we predict that high-temperature superconductivity is possible.

ACKNOWLEDGMENTS

We thank Tamio Oguchi for many helpful discussions and for his assistance with a number of calculations for the ferromagnetic phase using his LMTO program. We also thank Mei-Chun Huang for many valuable discussions and Mike Weinert for discussions about the hcp phase. This work was supported by the U.S. Air Force Office of Scientific Research (Grant No. 81-0024) and the U.S. Department of Energy.

[1] E. Wigner and H. B. Huntington, J. Chem. Phys. **3**, 764 (1935).
[2] N. W. Ashcroft, Phys. Rev. Lett. **21**, 1748 (1968); F. V. Grigor'ev, S. B. Kormer, O. I. Mikhailova, A. P. Tolochko, and V. D. Urlin, Pis'ma Zh. Eksp. Teor. Fiz. **16**, 286 (1972) [JETP Lett. **16**, 201 (1972)].
[3] R. P. Gupta and S. K. Sinha, in *Superconductivity in d- and f-Band Metals (Rochester)*, proceedings of the Conference on Superconductivity in *d*- and *f*-Band Metals, edited by D. H. Douglass (Plenum, New York, 1976), p. 583; D. A. Papaconstantopoulos and B. M. Klein, Ferroelectrics **16**, 307 (1977).
[4] L. F. Vereshchagin, E. N. Yakovlev, and Yu. A. Timofeev, Pis'ma Zh. Eksp. Teor. Fiz. **21**, 190 (1975) [JETP Lett. **21**, 85 (1975)].
[5] G. A. Neece, F. J. Rogers, and W. G. Hoover, J. Comput. Phys. **7**, 621 (1971); D. E. Ramaker, L. Kumar, and F. E. Harris, Phys. Rev. Lett. **34**, 812 (1975).
[6] J. Hammerberg and N. W. Ashcroft, Phys. Rev. B **9**, 409 (1974).
[7] S. Chakravarty, J. H. Rose, D. Wood, and N. W. Ashcroft, Phys. Rev. B **24**, 1624 (1981).
[8] J. H. Rose, H. B. Shore, and L. M. Sander, Phys. Rev. B **21**, 3037 (1980).
[9] E. Wimmer, H. Krakauer, M. Weinert, and A. J. Freeman, Phys. Rev. B **24**, 864 (1981).
[10] M. Weinert, E. Wimmer, and A. J. Freeman, Phys. Rev. B **26**, 4571 (1982); H. J. F. Jansen, A. J. Freeman, M. Weinert, and E. Wimmer, *ibid.* **28**, 593 (1983).
[11] H. J. F. Jansen and A. J. Freeman, Phys. Rev. B **30**, 561 (1984).
[12] G. D. Gaspari and B. L. Gyorffy, Phys. Rev. Lett. **28**, 801 (1972); D. A. Papaconstantopoulos, L. L. Boyer, B. M. Klein, A. R. Williams, V. L. Morruzzi, and J. F. Janak, Phys. Rev. B **15**, 4221 (1977).
[13] U. von Barth and L. Hedin, J. Phys. C **5**, 1629 (1972).
[14] L. Hedin and B. I. Lundqvist, J. Phys. C **4**, 2064 (1971).
[15] H. Nagara, H. Miyagi, and T. Nakamura, Prog. Theor. Phys. **56**, 396 (1976).
[16] P. Nozières and D. Pines, Phys. Rev. **111**, 442 (1958).
[17] O. K. Andersen, Phys. Rev. B **12**, 3060 (1975).
[18] C. A. Sholl, Proc. Phys. Soc. London **92**, 434 (1967).

[19]W. L. McMillan, Phys. Rev. **167**, 331 (1968).
[20]K. H. Benneman and J. W. Garland, in *Superconductivity in d- and f-Band Metals (Rochester)*, proceedings of the Conference on Superconductivity in *d*- and *f*-Band Metals, edited by D. H. Douglass (AIP, New York, 1972), p. 103.
[21]L. Caron, Phys. Rev. B **9**, 5025 (1974).
[22]T. Jarlborg and A. J. Freeman, Phys. Rev. B **22**, 2332 (1980).
[23]O. Gunnarsson and B. I. Lundqvist, Phys. Rev. B **13**, 4274 (1976).
[24]B. Sriram Shastry, Phys. Rev. **17**, 385 (1978).
[25]M. T. Yin and M. L. Cohen, Phys. Rev. Lett. **50**, 2006 (1983).
[26]W. Klement, Jr. and A. Jayaraman, Prog. Solid State Chem. **3**, 289 (1967).